Interaction of Triatomic Germanium with Lithium Atoms: Electronic Structure and Stability of Ge₃Liₙ Clusters

G. Gopakumar,[†] Peter Lievens,[‡] and Minh Tho Nguyen*[,†]

Department of Chemistry and Institute for Nanoscale Physics and Chemistry, University of Leuven, B-3001 Leuven, Belgium, and Laboratory of Solid State Physics and Magnetism and Institute for Nanoscale Physics and Chemistry, University of Leuven, B-3001 Leuven, Belgium

Quantum chemical calculations were applied to investigate the electronic structure of mono-, di-, and tri-lithiated triatomic germanium (Ge₃Liₙ) and their cations ($n = 0−3$). Computations using a multiconfigurational quasidegenerate perturbation approach (MCQDPT2) based on complete active space CASSCF wavefunctions, MRMP2 and density functional theory reveal that Ge₃Li has a $^2A'$ ground state with a doublet−quartet gap of 24 kcal/mol. Ge₃Li₂ has a singlet ground state with a singlet−triplet ($^3A''−^1A_1$) gap of 30 kcal/mol, and Ge₃Li₃ a doublet ground state with a doublet−quartet ($^4A''−^2A'$) separation of 16 kcal/mol. The cation Ge₃-Li⁺ has a $^1A'$ ground state, being 18 kcal/mol below the $^3A'$ state. The computed electron affinities for triatomic germanium are $EA_{(1)} = 2.2$ eV (experimental value is 2.23 eV), $EA_{(2)} = −2.5$ eV, and $EA_{(3)} = −5.9$ eV, for Ge₃⁻, Ge₃²⁻, and Ge₃³⁻, respectively, indicating that only the monoanion is stable with respect to electron detachment, in such a way that Ge₃Li is composed of Ge₃⁻Li⁺ ions. An atoms in molecules (AIM) analysis shows the absence of a Ge−Ge−Li ring critical point in Ge₃Li. An electron localization function (ELF) map of Ge₃Li supports the view that the Ge−Li bond is predominantly ionic; however, a small covalent character could be anticipated from the Laplacian at the Ge−Li bond critical point. The ionic picture of the Ge−Li bond is further supported by the natural bond orbital (NBO) results. The calculated Li affinity value for Ge₃ is 2.17 eV, and the Li⁺ cation affinity value for Ge₃⁻ amounts to 5.43 eV. The larger Li⁺ cation affinity of Ge₃⁻ favors an electron transfer, resulting in a Ge₃⁻Li⁺ interaction.

1. Introduction

The continuing interest in small elemental and molecular clusters[1,2] extends to the clusters of silicon and germanium and is anticipated due to their possible role in surface growth process and potential new applications in nanoelectronics. The presence of the coordinative unsaturation and dangling bonds is expected to be the main reason for the unusual physio-chemical properties shown by the gas-phase metal clusters. Experimental studies on small germanium clusters started in 1954 when Geₙ clusters containing two to eight atoms were first studied by Kohl.[3] A large number of both experimental[4−10] and theoretical[11−18] studies were reported thereafter. Mass spectra, atomization energies, photofragmentation, photoionization, photoelectron spectroscopy, electronic gaps, ion mobility measurements, etc., ... were the subject of the available experimental investigations. Knowledge about the structural identity of a cluster is important as the cluster properties, specifically, cluster relative stability and associated electronic structure, inherently depend on them. Due to this, most theoretical investigations focused mainly on the geometries, dissociation energies, electronic structures, and electron affinities. Relatively little attention has been paid to the properties of metal-doped Geₙ clusters.

On the other hand, the unusual structure, bonding mechanism, and reactions makes the organolithium compounds form a separate class. There has been considerable interest on the properties of these compounds, by both theoretical and experimental chemists alike.[19,20] The lithium atom in these compounds plays an important role and the characterization of the nature of the C−Li bond is still a matter of intense debate.[20] In this view, the interaction of germanium clusters with lithium, the simplest metal atom, is an emerging subject for both experimental and theoretical investigations. Recently, we reported a detailed investigation on the interaction of lithium with diatomic germanium (Ge₂).[21] In the present work, we set out to pursue the study investigating the electronic structure of lithium doped Ge₃ clusters based on our *ab initio* MO and density functional theory computations. Some key thermochemical parameters are derived, and the nature of the Ge−Li bonding in Ge₃Liₙ is further characterized.

2. Methods of Calculation

Our computations involve density functional theory (DFT) using the popular B3LYP functional in conjunction with the 6-311++G(d,p) basis set. As a preliminary step, the geometry optimizations were performed followed by the evaluation of the vibrational frequency analysis at the aforementioned level. The DFT computations were reconfirmed with the help of the ab initio molecular orbital (MO) theory, where a complete active space SCF (CASSCF) method has been applied. Given the fact that this method usually corrects for nondynamical or quaside-generate correlation effects with in the active space, the evaluation of dynamical correlation energies is, indeed, necessary for the description of states having multiconfigurational character.[22] For this purpose we have performed a perturbation

* Corresponding author. E-mail: minh.nguyen@chem.kuleuven.be. Fax: 32-16-32 7992.
† Department of Chemistry and Institute for Nanoscale Physics and Chemistry.
‡ Laboratory of Solid State Physics and Magnetism and Institute for Nanoscale Physics and Chemistry.

TABLE 1: Calculated Total and Relative Energies of Neutral Ge_3 and Its Mono-, Di-, and Trianions at the B3LYP/6-311++G(d,p), MRMP2/ECP,[a] and MCQDPT2/ECP[a] Levels

			total energy (rel energy) (kcal/mol)			
molecule	state	leading electronic configuration.	B3LYP[b]	CASSCF	MRMP2	MCQDPT2
Ge_3	$^1A_1$	...$2b_2^2$, $1b_1^2$, $3a_1^2$	−6231.0117 (0)	−10.9818 (0)	−11.1454 (0)	−11.1584 (0)
	$^3A_1'$	...$2b_2^1$, $1b_1^2$, $3a_1^2$, $4a_1^1$	−6231.0109 (0.5)	−10.9626 (12.1)	−11.1544 (−5.6)	−11.1304 (17.6)
Ge_3^-	$^2A_1$	...$2b_2^2$, $1b_1^2$, $3a_1^2$, $4a_1^1$	−6231.0919 (0)	−11.0220 (0)	−11.2210 (0)	−11.2251 (0)
	$^4B_2$	...$2b_2^2$, $3a_1^2$, $4a_1^1$, $1b_1^1$, $1a_2^1$	−6231.0346 (35.9)	−10.9676 (34.1)	−11.1658 (34.6)	−11.1810 (27.7)
Ge_3^{2-}	$^1A_1'$	...$3a_1^2$, $2b_2^2$, $4a_1^2$, $1b_1^2$	−6231.0018 (0)	−10.8995 (0)	−11.1146 (0)	−11.1167 (0)
	$^3\Sigma_g^-$	...$2\sigma_u^2$, $1\pi_u^4$, $1\sigma_g^2$	−6230.9844 (10.9)	−10.8976 (1.2)	−11.1072 (4.6)	−11.0791 (23.6)
Ge_3^{3-}	$^4\Sigma_u$	...$2\sigma_u^2$, $1\pi_u^4$, $1\pi_g^2$, $3\sigma_u^1$	−6230.7822 (0)	−10.6541 (0)	−10.8793 (0)	−10.8781 (0)
	$^2B_1$	...$3a_1^2$,$4a_1^2$,$2b_2^2$,$1b_1^2$,$2b_1^1$	−6230.7887 (−4.1)	−10.6220 (20.1)	−10.8542 (15.8)	−10.8781 (12.2)

[a] The effective core potentials adopted here are LANL2DZdp ECP for Ge. [b] The B3LYP total energy values are scaled by zero point energies at the same level.

analysis at multiconfigurational level, using the multiconfigurational quasidegenerate perturbation theory (MCQDPT2)[23] and the popular MRMP2[24] method. The former method usually provides corrected energies at second order for all states included in the model space simultaneously.[21] Throughout our MCQDPT2 analysis, an intruder state free technique has been adopted using a small energy denominator shift value to correct the "intruder states" problem.[25] In view of the finding that the LANL2DZdp basis set with an effective core potential (ECP) is good enough for the description of the quasidegenerate states in the Ge_2Li_n,[21] we have used the same basis set in the present study. The electronic structure of lithiated clusters are discussed in the following sections and, as a final step, an "atoms in molecules" (AIM) and "electron localization function" (ELF) analysis has been performed to characterize the Ge−Li bond. All computations, reported hereafter, were performed using the Gaussian 03,[26] GAMESS,[27] AIM2000,[28] and TopMod[29] suites of programs.

3. Results and Discussion

(a) Ge_3 and Its Anions. There has been considerable interest on triatomic germanium and its anions, whose ground electronic states are discussed in the most recent work of Xu et al.[30] Past experimental and theoretical studies[31] predicted a $^1A_1$ ground state for the triatomic germanium, with a lower-lying triplet $^3A_2'$ state. In agreement with the previous theoretical and experimental results, we derived a $^1A_1$ ground state for Ge_3. In our *ab initio* computations, in conjunction with a LANL2DZdp basis set, the 28 core-electrons on each germanium atom are modeled by an ECP. For the CASSCF computations, the 4s orbitals on each germanium atom were kept frozen, thus leading to a 6 electrons in 9 orbitals active space, referred to hereafter as CASSCF(6,9). The total energies are tabulated in Table 1, and the geometrical parameters are illustrated in Figure 1. The shape of the six active orbitals are illustrated in Figure 2 labeled under C_{2v} symmetry. Total energy values computed using the two different perturbation approaches, MRMP2 and MCQDPT2, are also listed in Table 1. The molecule exhibits a C_{2v} closed-shell singlet as the ground state. The leading electronic configuration has been derived as $^1A_1$:...$(2b_2)^2$ $(1b_1)^2$ $(3a_1)^2$ on the basis of CASSCF(6,9) computations. We were able to locate a quasidegenerate triplet state, $^3A_2'$ (D_{3h}), located at 0.5 kcal/mol above the closed-shell ground state $^1A_1$ at the B3LYP/6-311++G(d,p) level. The singlet−triplet transition induces a considerable change in geometry, the Ge−Ge bond lengths are increased by an amount of 0.2 Å, and the Ge−Ge−Ge bond angle is reduced by 20°. The leading electronic configuration, derived on the basis of our CASSCF(6,9) computation, is $^3A_2'$:...$(1b_1)^2$ $(3a_1)^2$ $(2b_2)^1$ $(4a_1)^1$. For comparison we have labeled the symmetry of the orbitals under C_{2v}; here the first symmetry
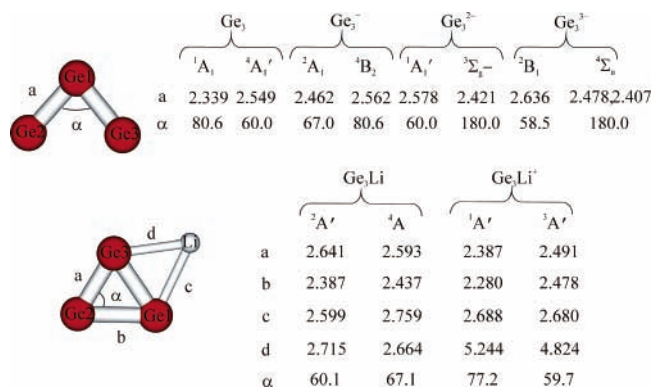

Figure 1. Selected CASSCF/ECP geometrical parameters of the Ge_3 (6,9), its anions, Ge_3Li (7,10) and Ge_3Li^+(6,10), considered in some lower-lying electronic states. Bond lengths are in angstrom and bond angles in degree.

plane has been chosen as the plane perpendicular to the molecular plane. Comparing with the ground electronic configuration, we can conclude that during the singlet−triplet transition the electronic excitation is from the $2b_2$ to the vacant $4a_1$ orbital. The $4a_1$ MO is bonding and acquires certain stabilization when the molecule undergoes the structural change from bent to cyclic. In other words, the occupancy of the electron in this bonding MO facilitates the geometrical change. At the CASSCF(6,9) level the calculated adiabatic excitation energy is on the order of 12 kcal/mol, but the MRMP2 predicted a reversed state ordering. It has been demonstrated[22] that special care should be taken when dealing with the quasidegenerate electronic states, where the MRMP2 method often fails. The MCQDPT2 method predicted the same state ordering as the CASSCF(6,9) calculations with a closed-shell singlet ground state, and an energy difference of the order of 17 kcal/mol.

Our previous computations on the interaction of diatomic germanium with lithium atoms indicated an electron transfer to the Ge_2 molecule.[21] Because of this obvious trend, it is, indeed, necessary to investigate the relative stability of the anions. Although many lower-lying doublet states have been predicted by DFT computations, our main interest was on the lowest-lying states of different spin manifolds. In the case of the Ge_3^- monoanion, in agreement with the past theoretical results, our computations predicted a $^2A_1$ (C_{2v}) ground state, followed by a lower-lying quartet $^4B_2$ state. For the lowest-lying states the leading electronic configurations based on our CASSCF(7,9) computation are $^2A_1$:...$(2b_2)^2$ $(1b_1)^2$ $(3a_1)^2$ $(4a_1)^1$ and $^4B_2$:...$(2b_2)^2$ $(3a_1)^2$ $(4a_1)^1$ $(1b_1)^1$ $(1a_2)^1$. During the doublet−quartet transition, the electron is moved from the doubly occupied $1b_1$ MO to the vacant $1a_2$ MO. Both these MOs are π-molecular orbitals, the former is a bonding MO, and the latter has a certain antibonding character. The geometrical changes
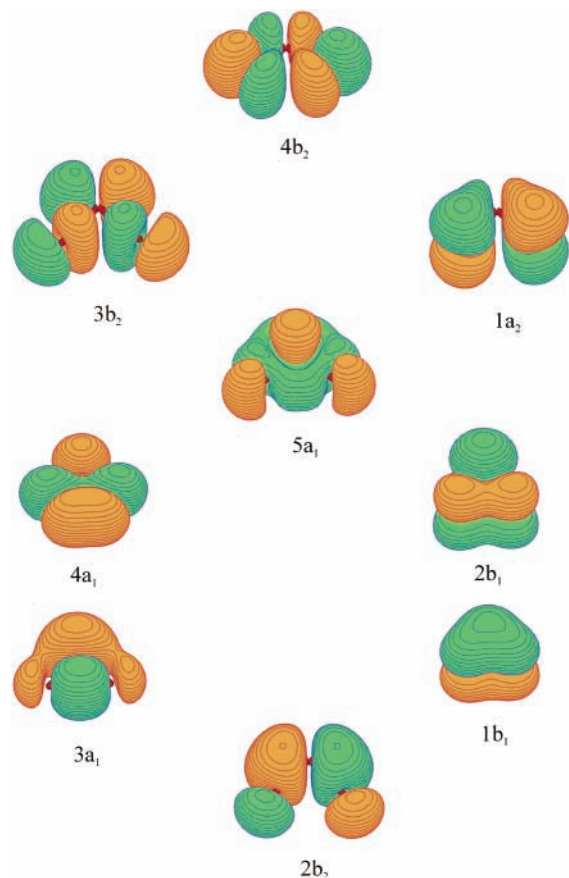
Figure 2. Shape of the nine natural orbitals of the Ge$_3$ and its anions selected for the CASSCF computations.

are significant during the doublet−quartet excitation, as the Ge−Ge bond lengths are increased by an amount of 0.1 Å and the bond angle opened by an amount of 13°. This could be anticipated because of the occupancy of the unpaired electron in 1a$_2$ MO, which has certain antibonding character. The B3LYP functional predicted a doublet−quartet gap of 36 kcal/mol, which is comparable with the CASSCF(7,9) value of 34 kcal/mol. The multireference perturbation approaches gave relatively comparable values, MRMP2 predicting 34.6 kcal/mol and a smaller gap of 28 kcal/mol by MCQDPT2.

For the Ge$_3{}^{2-}$ dianion we were able to locate a closed shell lowest-lying state with D_{3h} symmetry ($^1A_1{}'$). The lowest-lying triplet state, however, prefers a linear geometry ($^3\Sigma_g{}^-$). The UB3LYP method gave an energy difference of 11 kcal/mol but much smaller energy differences of the order of 1.2 kcal/mol and 4.6 kcal/mol were derived from CASSCF(8,9) and MRMP2 methods, respectively. The MCQDPT2 method predicted a large singlet−triplet gap of 23.6 kcal/mol. It could be noted that the MCQDPT2 method often gives a large gap when the geometries of the electronic states differ considerably from each other. In other words, in this case, the state averaging made by the CASSCF wavefunction is poorly balanced such that the second-order perturbation theory cannot fully recover the corresponding correlation. The only choice left is to increase the active space and to obtain a better state-averaged CASSCF wavefunction. Therefore, in the present case, we consider the value of 4.6 kcal/mol suggested by the MRMP2 method as a better result for the energy separation.

The leading electronic configurations of the singlet and triplet states are included in Table 1; for the sake of comparison, the MOs of the singlet state are labeled under the C_{2v} point group. The $^3\Sigma_g{}^-$ state results from the occupancy of the unpaired

electrons in the degenerate π_g orbitals, which are having some antibonding character and localized at the terminal germanium atoms. During the singlet−triplet excitation the 4b$_2$ and 1a$_2$ orbitals become singly occupied which are the degenerate π-MOs at linear geometry.

Subsequent addition of electrons leads to the formation of the Ge$_3{}^{3-}$ trianion which is having a lower-lying $^4\Sigma_u$ sate. UB3LYP calculations predicted a $^2B_1$ (C_{2v}) ground state, but our CASSCF(9,9) and multireference perturbation approaches predicted a reverse in state ordering. MRMP2 and MCQDPT2 levels predicted a gap of 16 and 12 kcal/mol, respectively, and a larger gap of 20 kcal/mol was predicted by CASSCF(9,9). In the case of the $C_{\infty v}$ symmetric $^4\Sigma_u$ state, the unpaired electrons occupy the degenerate $1\pi_g$ and the $3\sigma_u$ MOs. The quartet state is expected to be derived from the triplet state of the Ge$_3{}^{2-}$ dianion, by the electron addition to the vacant $3\sigma_u$ MO. In the case of the $^2B_1$ state (C_{2v}), the leading electronic configuration is similar to that of the dianion and the added electron occupies the 2b$_1$ π-MO. The electron affinities of triatomic germanium were calculated from the B3LYP energies using the following expressions:

$$EA_{(1)} = E(Ge_3) - E(Ge_3{}^-) \tag{1}$$

$$EA_{(2)} = E(Ge_3{}^-) - E(Ge_3{}^{2-}) \tag{2}$$

$$EA_{(3)} = E(Ge_3{}^{2-}) - E(Ge_3{}^{3-}) \tag{3}$$

The obtained values are EA$_{(1)}$ = 2.2 eV, EA$_{(2)}$ = −2.5 eV, and EA$_{(3)}$ = −5.9 eV. The computed electron affinity value for Ge$_3$ is in agreement with the experimental value of 2.23 eV.[31] Thus, the EA$_{(1)}$ value is positive and both EA$_{(2)}$ and EA$_{(3)}$ are negative, suggesting that only the Ge$_3{}^-$ monanion is apparently stable with respect to electron detachment.

(b) Ge$_3$Li. We have applied the same methodologies to investigate the interaction of lithium atoms with triatomic germanium. Preliminary geometric optimizations were performed with Gaussian 03 suites of programs at the B3LYP level using the unrestricted formalism in conjunction with 6-311++G(d,p) basis set. CASSCF and multireference perturbation computations were subsequently performed on these optimized geometries, but here we used the LANL2DZdp basis set. For the CASSCF optimizations the 4s orbitals of germanium atoms and 1s orbital of the lithium atoms were kept frozen. The active 10 orbitals include 4p orbitals of the three germanium atoms and the 2s orbital of lithium atoms, incorporating 7 electrons, referred to hereafter as CASSCF(7,10). Selected geometrical parameters for the doublet and quartet states of the neutral molecule are depicted in Figure 1, and the shapes of the 10 natural orbitals are illustrated in Figure 3, labeled under C_s symmetry, and include the 7 a′ and 3 a″ orbitals.

The lowest-lying electronic state of the lithium doped triatomic germanium was found to be $^2A'$. A nonsymmetric quartet state, ^4A, was located and is being energetically 24 kcal/mol above $^2A'$. At the CASSCF(7,10) level an energy gap of 28 kcal/mol was estimated with the doublet ground state. The difference in both doublet and quartet state geometries is large, irrespective of the fact that the elongation and shortening of Ge−Ge bond distances are by small amounts. In the quartet state, the lithium atom occupies the apex of the Ge$_3$ unit. Other differences include the Ge1−Li distance, which turns out to be increased by an amount of 0.16 Å and the Ge1−Ge2−Ge3 angle changes by 7°. The leading electronic configuration of the lower-lying electronic states along with the total energies at different
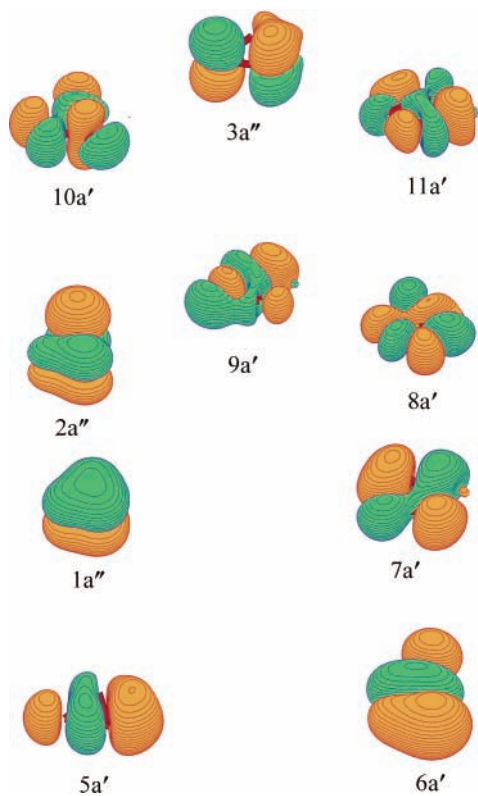
Figure 3. Shape of the ten natural orbitals of the Ge_3Li and its cation selected for the CASSCF computations.

levels is depicted in Table 2. In the ^4A state, the unpaired electrons occupy the MOs 7a, 8a, and 9a, which have the same shape as 5a′, 7a′, and 2a″ MOs labeled under C_s symmetry. The doublet−quartet excitation results from the promotion of the electron from the filled 5a′ to the vacant 2a″ MO. The multireference method MRMP2 gave a smaller gap of 24 kcal/mol, and the MCQDPT2 predicted a much larger gap of 46.7 kcal/mol. Again, this large energy difference could be due to the large difference in the doublet−quartet geometries, and the inadequacies of the state-averaged CASSCF wavefunction. As demonstrated earlier in the case of $Ge_3{}^{2-}$ dianion, in such cases, caution must be taken while comparing the MCQDPT2 results.

Removal of an electron from the Ge_3Li leads to the formation of Ge_3Li^+ cation, which has a closed shell singlet ground state. Here, the lithium atom connects to one of the terminal germanium atoms of Ge_3 unit and structurally falls under C_s symmetry, and the electronic state is assigned to $^1A′$. On the basis of our CASSCF(6,10) computations, we were able to derive a lowest-lying triplet state, $^3A′$, with the same symmetry. The singlet−triplet gap is estimated to 1 kcal/mol at the UB3LYP/6-311++G(d,p) level, but CASSCF(6,10) computations predicted a larger gap of 11 kcal/mol. Computations of electronic states having multiconfigurational character demands an appropriate evaluation of the dynamic correlation energy. In this case, the MRMP2 method predicted a reversed state ordering with a singlet−triplet gap of −3.5 kcal/mol and the MCQDPT2 computations were in agreement with CASSCF(6,10) computation and suggested a gap of 18 kcal/mol. The separate application of the perturbative treatements to quasidegenerate electronic states can sometimes lead to a reverse in state ordering, where often a root flipping occurs, or the perturbation series diverges due to the existence of intruder states.[25] It has been proven that in these cases, MCQDPT2 computations are more effective when an intruder-state-free technique is used. Therefore, in this case, the singlet−triplet

gap of 18 kcal/mol predicted by the MCQDPT2 method is a more reliable result.

Examination of the CI coefficients suggests a predominant electronic configuration, $^1A′:...(5a′)^2$ $(6a′)^2$ $(1a″)^2$ and $^3A′:...(5a′)^2 (6a′)^1 (1a″)^2 (7a′)^1$. It is clear that the singlet−triplet transition accompanies an electronic jump from the filled 6a′ MO to the vacant 7a′ MO of ^1A. Both MOs are of σ type and the geometrical change during the transition is apparent and is due to the bonding interaction of the 7a′ MO, which facilitates a cyclic geometry. An energy difference of 151.2 kcal/mol has been calculated between the ground states of the neutral and the cation, indicating an ionization energy of $IE(Ge_3Li) = 6.6$ eV, which is small compared to that of 7.8 eV of Ge_3, but closer to that of 5.39 eV for the lithium atom. A similar trend was observed for the interaction of lithium atoms with diatomic germanium.[21] Due to its presence, attachment of lithium tends to lower the IE of the doped cluster and thereby facilitates the electron removal.

(c) Ge_3Li_2 and Ge_3Li_3. Progressive addition of lithium atoms to Ge_3Li yields Ge_3Li_2 and Ge_3Li_3. For the MO computations of Ge_3Li_2 an 8-electrons-in-11-orbitals active space has been chosen, referred to hereafter as CASSCF(8,11). The aforementioned active space includes the 4p orbitals of germanium atoms and the 2s orbitals of lithium atoms. The 4s orbitals of germanium atoms and the 1s orbital of lithium is kept frozen, and the 28 core electrons of germanium atoms has been modeled using an effective core potential. Optimized geometries and selected geometrical parameters of the two lower-lying electronic states of the neutral Ge_3Li_2 are illustrated in Figure 4, whereas the total and releative energies at different levels and the leading electronic configurations based on the CASSCF-(8,11) computations are listed in Table 2. Preliminary geometry optimizations were performed at the DFT level, and a C_{2v} symmetric ground state has been derived for the Ge_3Li_2.

The C_{2v} closed-shell singlet ground state, $^1A_1$, lies energetically 30 kcal/mol below the triplet $^3A″$ state (C_s) at the B3LYP/6-311++G(d,p) level. CASSCF(8,11) calculations predicted an energy gap of 33 kcal/mol, the MRMP2 method suggested a gap of 30 kcal/mol, but the MCQDPT2 method results in a larger gap of 43 kcal/mol. A closer examination of the singlet and triplet geometries suggests a large geometrical difference, in the latter the lithium atoms are situated above and below the plane of the molecule. As stated earlier, when there is a large difference in geometries the relative energy values suggested by MCQDPT2 should be handled with caution. Therefore, in this case, we consider the MRMP2 energy difference value as more reliable, and the singlet−triplet energy gap could be predicted to be of the order of 30 kcal/mol. CI coefficients suggest that these two states have the following leading electronic configurations, $^1A_1:...(4a_1)^2$ $(3b_2)^2$ $(5a_1)^2$ $(1b_1)^2$ and $^3A″:...(5a′)^2 (2a″)^2 (6a′)^2 (3a″)^2 (7a′)^1$.

Removal of an electron from the Ge_3Li_2 leads to the formation of the cation, $Ge_3Li_2^+$ which possesses a doublet ground state $^2A_1$, whose geometry is relatively similar to that of the neutral ground state. The leading electronic configuration based on the CASSCF(7,11) computation is $^2A_1:...(4a_1)^2 (3b_2)^2 (1b_1)^2 (5a_1)^1$. Comparison with the ground state electronic configuration of the neutral molecule enables us to conclude that the removal of the electron occurs from the filled 5a1 MO, which is a σ-type orbital. A lowest-lying quartet state $^4A″$ has been derived on the basis of DFT computations and is confirmed by MO methods. A doublet−quartet gap of 27 kcal/mol is predicted by DFT, CASSCF(7,11), and MRMP2 methods. Again, the MCQDPT2 energy difference of 53.5 kcal/mol is large and not

TABLE 2: Calculated Total and Relative Energies of Mono-, Di- and Tri- Lithiated Triatomic Germanium and Its Cations at B3LYP/6-311++G(d,p) and MCQDPT2/ECP^a Level

molecule	state	leading electronic configuration	total energy (rel energy) (kcal/mol)			
			B3LYP^b	CASSCF	MRMP2	MCQDPT2
Ge$_3$Li	^{2}A'	...5a'^{2}, 6a'^{2}, 1a''^{2}, 7a'^{1}	−6238.5800 (0)	−18.4660 (0)	−18.6602 (0)	−18.6684 (0)
	^{4}A	...5a^2, 6a^2, 7a^1, 8a^1, 9a^1	−6238.5408 (24.6)	−18.4212 (28.1)	−18.6223 (23.8)	−18.5939 (46.7)
Ge$_3$Li$^+$	^{1}A'	...5a'^{2}, 6a'^{2}, 1a''^{2}	−6238.3391 (0)	−18.2644 (0)	−18.4236 (0)	−18.4301 (0)
	^{3}A'	...5a''^{2}, 6a'^{1}, 1a''^{2}, 7a'^{1}	−6238.3375 (1.0)	−18.2472 (10.8)	−18.4292 (−3.5)	−18.4012 (18.1)
Ge$_3$Li$_2$	^{1}A$_1$	...4a$_1^2$, 3b$_2^2$, 5a$_1^2$, 1b$_1^2$	−6246.1628 (0)	−25.9782 (0)	−26.1752 (0)	−26.1834 (0)
	^{3}A'' (D_{2h})	...5a'^{2}, 2a''^{2}, 6a'^{2}, 3a''^{1}, 7a'^{1}	−6246.1162 (29.2)	−25.9257 (32.9)	−26.1276 (29.9)	−26.1149 (42.9)
Ge$_3$Li$_2^+$	^{2}A$_1$	...4a$_1^2$,3b$_2^2$,1b$_1^2$,5a$_1^1$	−6245.9335 (0)	−25.7678 (0)	−25.9568 (0)	−25.9678 (0)
	^{4}A'' (C_s)	...5a'^{2}, 2a''^{2}, 6a'^{1}, 3a''^{1}, 7a'^{1}	−6245.8894 (27.7)	−25.7252 (26.7)	−25 09146 (26.5)	−25.8826 (53.5)
Ge$_3$Li$_3$	^{2}A'	...3a''^{2}, 5a'^{2}, 6a'^{2}, 7a'^{2}, 8a'^{1}	−6253.6912 (0)	−33.4289 (0)	−33.6346 (0)	−33.6407 (0)
	^{4}A''	...2a''^{2}, 6a'^{2}, 7a'^{2}, 3a''^{1}, 4a''^{1}, 8a'^{1}	−6253.6559 (22.2)	−33.3808 (30.2)	−33.6088 (16.2)	−33.5618 (49.5)
Ge$_3$Li$_3^+$	^{1}A$_1$	...5a$_1^2$, 3b$_2^2$, 6a$_1^2$, 1b$_1^2$	−6253.5402 (0)	−33.3078 (0)	−33.4949 (0)	−33.5065 (0)
	^{3}A''	...3a''^{2}, 5a'^{2}, 6a'^{2}, 4a''^{1}, 7a'^{1}	−6253.4820 (36.5)	−33.2371 (44.4)	−33.4451 (31.2)	−33.4252 (51.0)

^{a} The effective core potentials adopted here are LANL2DZdp ECP for Ge. The LANL2DZ basis set is implemented for lithium atoms. ^{b} The B3LYP total energy values are scaled by zero point energies at the same level.
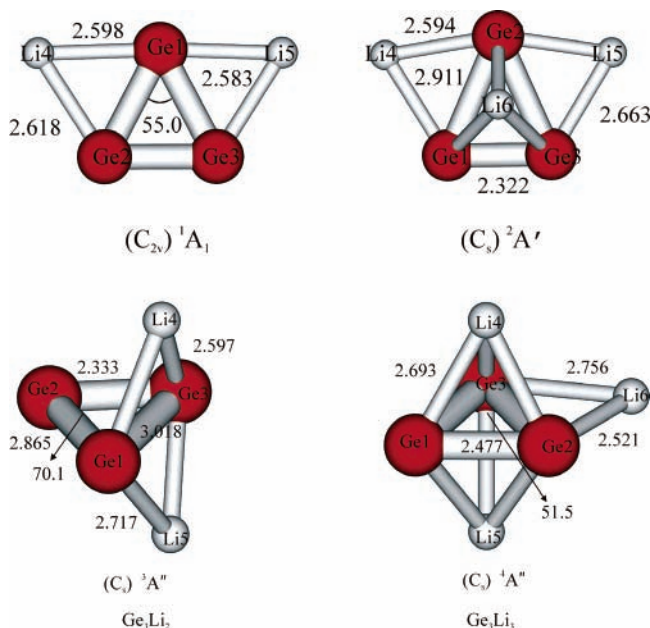

Figure 4. Selected CASSCF/ECP geometrical parameters of Ge$_3$Li$_2$ (8,11) and Ge$_3$Li$_3$ (9,12) considered in some lower-lying electronic states. Bond lengths are in angstroms and bond angles in degrees.

reasonable, owing to the large difference in the geometries of the considered electronic states.

Further lithiation on Ge$_3$Li$_2$ yields Ge$_3$Li$_3$, which is having a doublet ground state, ^{2}A'. Selected geometrical parameters of the two lowest-lying states are shown in Figure 4 and the total and relative energies at different levels are listed in Table 2. Addition of the third lithium prefers the apex of the triatomic germanium unit. A doublet−quartet gap of 22 kcal/mol is estimated on the basis of DFT computations, but a larger gap of 30 kcal/mol is predicted by the CASSCF(9,12) computations. The MRMP2 method predicted a small gap of 16 kcal/mol and the MCQDPT2 predicted a larger gap of 50 kcal/mol. The quartet state differs much from the lowest-lying doublet state and is very similar to the quartet ^{4}A'' state of Ge$_3$Li$_2^+$, where the two lithium atoms occupy the apex of a Ge$_3$ unit and the third lithium bridges two germanium atoms. The leading electronic configurations for the two states are derived to be ^{2}A':...(3a'')^2 (5a')^2 (6a')^2 (7a')^2 (8a')^1 and ^{4}A'': ...(2a'')^2 (6a')^2 (7a')^2 (3a'')^1 (4a'')^1 (8a')^1.

Removal of an electron from the trilithiated species results in the Ge$_3$Li$_3^+$ cation, and it exhibits a closed-shell singlet ground state ^{1}A$_1$ (C_{2v}). A lowest-lying triplet ^{3}A'' state has been

located 36 kcal/mol above the singlet (B3LYP). A relatively larger energy gap of 44 kcal/mol has been predicted by the CASSCF(8,12) computation, whereas MRMP2 predicted a lower gap of 31 kcal/mol. The singlet and triplet state differ much from each other in their geometries. For ^{1}A$_1$, all three lithium atoms are in the plane surrounding the cyclic Ge$_3$ unit, whereas in the ^{3}A'' state one lithium atom occupies the apex position. Due to this fact, the large MCQDPT2 value is not a reasonable one compared to the MRMP2 gap. The leading electronic configurations for the two states are ^{1}A$_1$: ...(5a$_1$)^2 (3b$_2$)^2 (6a$_1$)^2 (1b$_1$)^2 and ^{3}A'': ...(3a'')^2 (5a')^2 (6a')^2 (4a'')^1 (7a')^1.

On the basis of the total energies, we were able to calculate the Li$^+$ cation affinity (denoted as Li$^+$A) of Ge$_3^-$ and the lithium affinity (LiA) of Ge$_3$ using the following equations:

$$\text{Li}^+\text{A}(\text{Ge}_3^-) = -[E(\text{Ge}_3\text{Li}) - \{E(\text{Ge}_3^-) + E(\text{Li}^+)\}] \qquad (4)$$

$$\text{LiA}(\text{Ge}_3) = -[E(\text{Ge}_3\text{Li}) - \{E(\text{Ge}_3) + E(\text{Li})\}] \qquad (5)$$

The lithium affinity could be considered as a measure of the degree of stabilization attained by the molecule upon lithiation. According to the present definition, a positive lithium affinity corresponds to stabilization, whereas a negative value indicates a destabilization. In the present case, the calculated Li$^+$ cation affinities are positive, suggesting that the doped molecule attains certain stability upon lithiation. For Ge$_3$, the calculated lithium affinity value is 2.17 eV and, indeed, smaller than the Li$^+$ cation affinity of the Ge$_3^-$ anion, which amounts to 5.43 eV. The large Li$^+$ cation affinity of Ge$_3^-$ thus favors an electron-transfer resulting in a Ge$_3^-$Li$^+$ interaction. These values show the same trend as in the case of Ge$_2$Li.[21] It is also important to consider the basis set superposition error (BSSE) for the computed lithium affinity values. In the present work, the aforementioned lithium affinity values are corrected for BSSE, measured using the counterpoise methodology.

In summary, we have analyzed the electronic structure of mono-, di-, and trilithiated triatomic germanium on the basis of DFT and MO computations. The interest of the role of lithium in stabilizing the molecule demands a further look at the problem. Here we adopted two different methodologies, namely, the atoms in molecules (AIM) and electron localization function (ELF) analysis, on some systems to investigate the nature of Ge−Li bond. A parallel natural bond orbital (NBO) computation was also performed and is discussed in the following section.

(d) Nature of the Ge−Li Bond. The AIM concept is a useful tool providing valuable information about the structure and
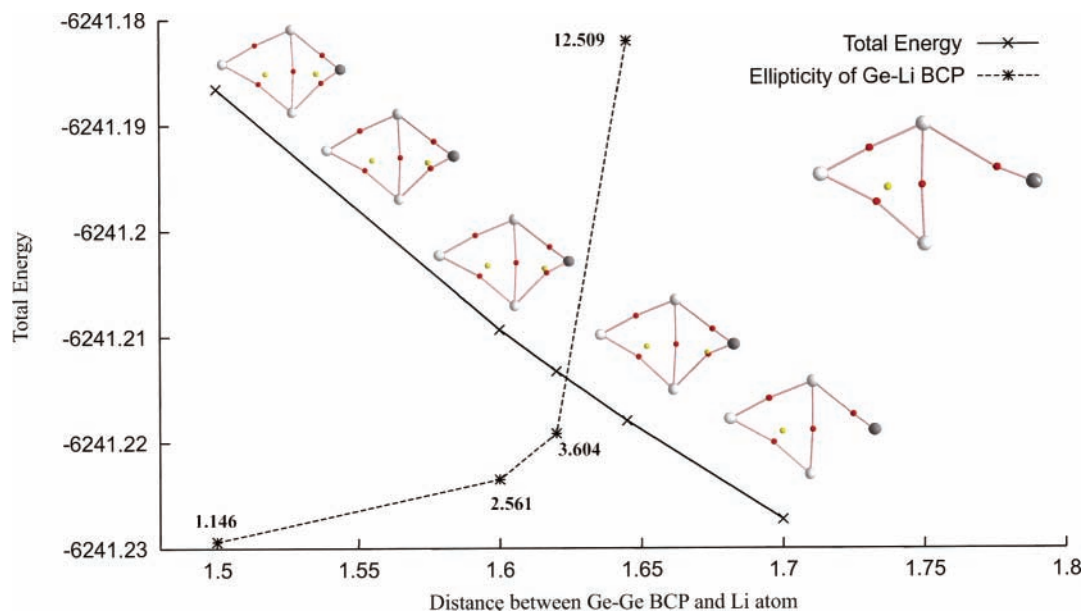
Figure 5. Energy profile, for the bifurcation mechanism, as a function of the distance between lithium atom and the Ge−Ge geometric center. The top right corner represents the resolved structure of the conflict mechanism. The dotted lines indicate the ellipticity of the Ge−Li bond critical point at different distances.

bonding in molecules.[32,33] AIM has thus been used to investigate the structure and bonding in traditional organolithium compounds and even supports the ionic nature of the C−Li bond.[34] According to the AIM theory, a critical point (cp), where the gradient of the electron density vanishes, holds chemical information and allows us to define atoms and chemical bonds within a molecule. The main questions that we considered here were: (i) Is there a bond connecting the two germanium atoms and lithium? Otherwise stated, is the lithium atom really bridging the Ge_3 molecule? (ii) Ultimately, what is the nature of the Ge−Li bond?

The wavefunction files used for the AIM analysis were generated at the B3LYP level in conjunction with the 6-311G** basis set using the GAMESS suite of programs. Then, the critical points were located and the bond paths were plotted using the AIM2000 suite of programs. Interestingly, for Ge_3Li we were not able to locate a Ge−Ge−Li ring critical point, i.e., the part of the molecular graph that bounds a ring surface. The molecular graph of Ge_3Li comprises four bond critical points (bcp), one ring critical point (rcp) and four attractors, i.e., the nuclei (cf. Figure 5 top right corner).

The ellipticity, a quantity defined as

$$\epsilon = (\lambda_1/\lambda_2 - 1) \qquad \lambda \leq \lambda_2 \leq \lambda_3$$

where λ_1, λ_2, and λ_3 are the eigenvalues of the Hessian, measures the behavior of the electron density at a given point, in the plane tangential to the interatomic surface. The ellipticity value ranges from zero to infinity and is widely regarded as a quantitative index of the π-character of the bond. The bcp connecting Ge1 and Ge3 atoms has an ellipticity value of 0.62, suggesting a certain π-character to the Ge1−Ge3 bond. This is in agreement with MO calculations, where the leading electronic configuration suggests a completely filled $1a''$ MO. The bcp between Ge and Li lies close to the lithium atom and has an ellipticity of 0.67, which is smaller compared to the value of 0.87 in Ge_2Li.[21]

Figure 5 (top right corner) represents a molecular graph of Ge_3Li. Any motion of Li close to the Ge_3 unit will give rise to a bifurcation mechanism.[32,33] To illustrate this point, we plotted

TABLE 3: Calculated Elipticity of Ge−Li Bond Critical Points at Different Geometries, for the Potential Energy Profile of the Bifurcation Mechanism

distance between the Li and Ge−Ge geometric center (Å)		elipticity[a]
1.5	1.146	0.356
1.6	2.561	0.373
1.62	3.604	0.378
1.63	4.693	0.380
1.64	7.417	0.383
1.645	12.509	0.384
minima		0.671

[a] Values corresponds to the bond critical points in the Ge−Li bond path.

the energy profile as a function of the distance between Li and the Ge1−Ge3 geometric center, generating the molecular graphs at each point. At a distance of 1.5 Å between the Li and the Ge1−Ge3 geometric center, there exists a rcp; at this geometry, the lithium atom behaves as a bridging entity. Upon increasing this distance, the rcp merges with one of the Ge−Li bcps as expected in a bifurcation mechanism (cf. Figure 5). This bifurcation mechanism is different from the one observed in Ge_2Li where both of the Ge−Li bcps were found to merge with the nearby rcp.[21] At a distance of 1.65 Å, the rcp annihilates upon uniting with one of the Ge−Li bcps. Interestingly, for Ge_2-Li this resulted in a conflict structure that was resolved by an infinitesimal distortion of Li leading to the global minimum. In the present system, the bifurcation mechanism appears different in this respect. It is interesting to note the behavior of the ellipticity of Ge−Li bcp (the one participating in the annihilation) following the bifurcation mechanism. The relevant values are also plotted in Figure 5 using dotted lines and also listed in Table 3 along with the ellipticities. At the geometric energy minimum, the elipticity of the Ge−Li bcp becomes 0.67.

Analysis of the Ge−Li bcp is expected to provide more information about the nature of the Ge−Li bond. With this goal in mind, we evaluated the charge density (ρ_b), Laplacian (L_b), and the ellipticity (ϵ) at the Ge−Li bcps in a series of relevant compounds, and the results are summarized in Table 4. The

Interaction of Ge$_3$ with Li

J. Phys. Chem. A, Vol. 111, No. 20, 2007 **4359**

TABLE 4: Charge Density (ρ_b), Laplacian (L_b), and Ellipticity (ϵ) Calculated at the Bond Critical Point between Ge and Li Atoms in Different Molecules

molecule	charge density at bond critical point (ρ_b)	Laplacian of ρ at bond critical point (L_b)	ellipticity (ϵ) at bond critical point
GeLi^a	0.021	0.014	0.0
GeLi$_2$^{a}	0.022	0.014	0.0
GeLi$_3$^{a}	0.026	0.021	0.080
Ge$_2$Li^a	0.023	0.011	0.865
Ge$_2$Li$_2$^{a}	0.022	0.015	0.663
Ge$_2$Li$_3$^{a}	0.022	0.019	0.744
Ge$_3$Li	0.024	0.016	0.671
Ge$_3$Li$_2$	0.021	0.015	1.571

^{a} Values taken from ref 21.

electron density Laplacian, measured at a bcp and defined as $L_b = \nabla^2\rho_{bcp}$, usually helps us to understand the nature of the bond involved. Accordingly, a value of $L_b < 0$ indicates a closed-shell interaction (i.e., the charge is predominantly contracted toward each of the nuclei), whereas a positive value ($L_b > 0$) suggests a shared interaction (i.e., the electronic charge is concentrated in the internuclear region). According to the above definition, ionic bonds, bonds in van der Waals molecules and noble gas clusters are all closed interactions. In contrast, covalent or polar bonds are shared interactions. In the former, mostly, the electron density at the bond critical point will be low, of the order of 10^{-2}, whereas in the latter, it will be of the order of 10^{-1}.

Examination of the electron density values in compounds ranging from Ge−Li to Ge$_3$Li$_3$ suggests that they maintain constant and lower values. In the case of Ge−Li and GeLi$_2$, the ellipticity values are found to be close to zero, indicating a certain σ-type bond between the Ge and Li atoms. In the compounds ranging from Ge$_2$Li to Ge$_3$Li$_2$, the ellipticity values are larger, indicating certain π-character to the corresponding Ge−Li bond. Note that in the present system, the evaluated electron density values are too low with small positive L_b values. This leads us to a conclusion that the Ge−Li bond has a very small covalent character.

For additional insights, we performed ELF and NBO analyses on these molecules. The ELF is a simple measure of the electron localization in atomic and molecular systems.[35] The ELF values are always in a range of [0;1] and relatively large where the electrons are unpaired or formed into pairs with antiparallel spins. The zero flux surfaces of the ELF separate the electron density space into basins (Ω_i), thus helping us define and calculate the properties of core, chemical bond, and lone pairs.[35] The corresponding basins are mainly classified into two types, i.e., core and valence basins. Although the former are mainly located around the nuclei and always occur when the atomic number is larger than 2, the latter are characterized by their synaptic orders, i.e., the number of the core basins that share a common boundary surface with the valance basin. Monosynaptic basins represent the lone pairs and the disynaptic basins belong to the covalent bonds. The integral of the electron density over Ω_i shows the population of the given basin.

The calculations were performed using the TopMod suites of programs and the ELF isosurfaces were visualized using the gOpenMOL software.[36] The ELF isosurfaces and their cut planes of Ge$_3$, Ge$_3$$^-$ anion and Ge$_3$Li are illustrated in Figure 6. The mean electronic populations computed for the basins localized for each molecule are summarized in Table 6. The mean electronic populations of some model systems, from previous computations,[21,37] are also included. Finally, for the sake of comparison we also performed an NBO analysis at the
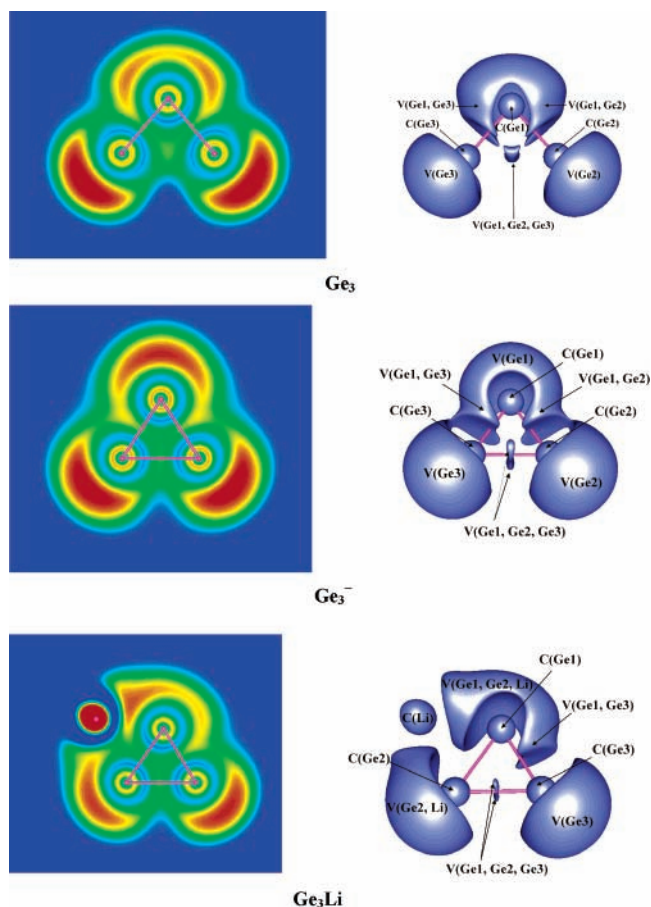

Figure 6. Cut planes and ELF isosurfaces of Ge$_3$, Ge$_3$$^-$, and Ge$_3$Li ($\eta = 0.6$).

UB3LYP/6-311++G(d,p) level and the obtained results are listed in Table 5 along with the data available in the literature.

A discussion on the ELF results for GeLi$_n$ ($n = 1−4$), Ge$_2$, the Ge$_2$$^-$ anion, and Ge$_2$Li can be found elsewhere.[21] In the present work we focus mainly on the nature of the Ge−Li bond in Ge$_3$Li. The ELF isosurfaces and the cut planes for Ge$_3$, its anion, and Ge$_3$Li are illustrated in Figure 6.

In the case of Ge$_3$, our computations suggest the presence of two V(Ge) basins, which could be regarded as the lone pair basins of germanium atoms, each having an electronic population of 2.68 electrons. For the C(Ge) basins the electronic population is computed to be 27.59 electrons. There also exist two V(Ge,Ge) basins each having an electronic population of 3.15 electrons, which is less than 4.27 electrons computed for the Ge$_2$ system reported in the our previous work.[21] We were also able to locate a trisynaptic basin V(Ge1,Ge2,Ge3) with an electronic population of 1.58 electrons, indicating a certain three-center bond between the germanium atoms. The ELF isosurface of Ge$_3$$^-$ anion is quite different from the neutral counter part; here we were able to locate three V(Ge) basins, i.e., the lone pair basins, with an electronic population of 2.91 electrons each. This value is smaller than the one computed for the neutral conterpart but closer to the value of 3.05 electrons computed for the Ge$_2$$^-$ anion. The V(Ge,Ge) basin population is reduced to 1.92 whereas the C(Ge) basin population remains almost unchanged with respect to that of neutral Ge$_3$. Similar to the case of the neutral conterpart, we were also able to locate two trisynaptic basins each having a population of 0.75 electrons.

The ELF picture of Ge$_3$Li is almost similar in shape to that of the Ge$_3$$^-$ anion. Accordingly, there are two trisynaptic basins,

TABLE 5: Calculated Wiberg Indices (*Wi*) and NBO Charges of Various Germanium−Lithium Complexes at B3LYP/ 6-311++G(d,p) Level

	Wiberg indices (*Wi*)				NBO charges (au)			
molecule	Ge1−Ge2	Ge2−Ge3	Ge1−Ge3	Ge−Li	Ge1	Ge2	Ge3	Li
GeLi[b]				0.24	−0.76			0.76
GeLi$_2$[b]				0.37	−1.54			0.77
GeLi$_3$[a,b]				0.34	−2.41			0.80
GeLi$_4$[b]				0.29	−3.37			0.84
GeLi$_5$[b]				0.25, 0.5	−3.06			0.66, 0.41
GeLi$_6$[b]				0.15	−3.65			0.61
Ge$_3$	1.73	0.77	1.73		−0.44	0.22	0.22	
Ge$_3^-$	1.45	0.99	1.45		−0.46	−0.27	−0.27	
Ge$_3$Li	1.45	0.958	1.35	0.13	−0.58	0.08	−0.33	0.84
Ge$_3$Li$_2$	1.33	1.45	1.33	0.12, 0.11	−0.90	−0.39	−0.39	0.84
Ge$_3$Li$_3$	0.844	0.843	1.865	0.11, 0.14, 0.12	−0.57	−1.26	−0.57	0.82, 0.76

[a] At B3LYP level this structure has two imaginary frequencies corresponding to the elongation of one of the Ge−Li bonds having magnitudes 28.3 and 19.8 cm^{-1}, respectively. [b] Values taken from ref 21.

TABLE 6: Mean Electronic Populations Computed for Basins Localized in GeLi$_n$ (*n* = 1−4) and Ge$_3$Li

	basins						
molecule	C(Ge)[a]	C(Li)	V(Ge)	V(Ge,Ge)	V(Ge,Li)	V(Ge,Ge,Li)	V(Ge,Ge,Ge)
GeLi[b]	27.61	2.03	2.12		3.15		
GeLi$_2$[b]	27.57	2.02			3.17		
GeLi$_3$[b]	27.51	2.02			1.22		
GeLi$_4$[b]	27.61	2.03				2.05	
Ge$_3$	27.59		2.68	3.15			1.58
Ge$_3^-$	27.58		2.91	1.92			0.75
Ge$_3$Li	27.54	2.02	2.85	2.84	3.23	3.52	0.95

[a] Sum of all core basins of Ge. [b] Values taken from ref 21.

located above and below the plane of the molecule, each having an electronic population of 0.95 electrons. Note that this value is comparable to that of the same in the Ge$_3^-$ anion. A trisynaptic V(Ge,Ge,Li) basin was also located, having an electronic population of 3.52 electrons (the V(Ge,Li) basin has also a similar population). Owing to the similarities of the shape of the basins and the comparable electronic populations, a Ge$_3^-$ and Li$^+$ interaction could be anticipated.

In the case of Ge$_3$, Wiberg indices indicate a bond order of 1.45 between Ge1−Ge2 and Ge1−Ge3, whereas it is 0.99 between Ge1−Ge3. The bond index values are almost the same in Ge$_3$Li; the Ge−Li bond index being 0.13, and smaller than that computed for Ge$_2$Li, suggesting a weak bond. In the case of Ge$_3$Li$_2$ and Ge$_3$Li$_3$, we observed a similar order in bond index. For Ge$_3$Li, the computed NBO charges indicate a certain negative charge on the germanium atoms and a positive charge on the lithium atom. Both the ELF and NBO results tend thus to support a certain ionic character of the Ge−Li bond. Similar trends are also observed in Ge$_3$Li$_2$ and Ge$_3$Li$_3$, where the NBO charge calculations point out an ionic picture of Ge−Li bond in both molecules.

4. Concluding Remarks

In summary, we have analyzed the electronic structure of mono-, di-, and trilithiated Ge$_3$ and their cations. Our quantum chemical computations allow the following conclusions to be drawn.

(i) For Ge$_3$Li, a doublet ^{2}A′ ground state is confirmed with a doublet−quartet electronic gap of 24 kcal/mol (at the MRMP2/ ECP level).

(ii) The Ge$_3$Li$^+$ cation has a closed-shell singlet ground state, and a singlet−triplet gap of 18 kcal/mol is derived on the basis of the MCQDPT2/ECP computations.

(iii) Density functional thieory computations with (U)B3LYP functional are in qualitative agreement with our MO results.

(iv) The calculated electron affinities of diatomic germanium amount to EA$_{(1)}$ = 2.2 eV, EA$_{(2)}$= −2.5 eV, and EA$_{(3)}$ = −5.9 eV, and only Ge$_3^-$ anion is likely to be stable with respect to electron detachment. The EA$_{(1)}$ value compares well with the experimental result of 2.23 eV (ref 31).

(v) The larger Li$^+$ cation affinity value of Ge$_3^-$ (compared to the lithium affinity value of Ge$_3$) supports a Ge$_3^-$Li$^+$ interaction.

(vi) The AIM approach reveals the absence of a Ge−Ge−Li ring critical point.

(vii) The ELF and NBO analyses lead us to the conclusion that the Ge−Li bond is predominantly ionic.

(viii) Our MO computations indicate that much caution must be taken when using the MCQDPT2 method for the electronic states that differ much from each other in their geometries.

We would anticipate that the design of alkali metal doped germanium clusters is an emerging subject for experimental research and hope that the present computational results, along with our previous work on Ge$_2$Li$_n$,[21] provide some useful insights into the electronic structure of larger lithium doped germanium clusters.

References and Notes

(1) Jarrold, M. F. *Science* **1991**, *252* (5009), 1085.
(2) Raghavachari K.; Curtiss, L. A. In *Quantum mechanical electronic structure calculations with chemical accuracy*; 1995.
(3) Kohl, V. G. Z. *Naturforsch. B* **1954**, *9A*, 913.
(4) Arnold, C. C.; Xu, C.; Burton, G. R.; Neumark, D. M. *J. Chem. Phys.* **1995**, *102*, 6982.
(5) Burton, G. R.; Xu, C.; Arnold, C.; Neumark, D. M. *J. Chem. Phys.* **1996**, *104*, 2757. Burton, G. R.; Xu, C.; Neumark, D. M. *Surf. Rev. Lett.* **1996**, *3*, 383.

(6) Cheshnovsky, O.; Yang, S. H.; Pettiette, C. L.; Craycraft, M. J.; Liu, Y.; Smalley, R. E. *Chem. Phys. Lett.* **1987**, *138*, 119.

(7) Gingerich, K. A.; Finkbeiner, H. C.; Schmude, R. W., Jr. *J. Am. Chem. Soc.* **1994**, *116*, 3884. Gingerish, K. A.; Shim, I.; Guptha, S. K.; Kingcade, J. E. *Surf. Sci.* **1985**, *156,* 495.

(8) Kingcade, J. E.; Choudary, U. V.; Gingerish, K. A. *Inorg. Chem.* **1979**, *18*, 3094.

(9) Negishi, Y.; Kawamata, H.; Hayase, T.; Gomei, M.; Kishi, R.; Hayakawa, F.; Nakajima, A.; Kaya, K. *Chem. Phys. Lett.* **1997**, *269*, 199.

(10) Xu, C.; Taylor, T. R.; Burton, G. R.; Neumark, D. M. *J. Chem. Phys.* **1998**, *108*, 1395.

(11) Jackson, P.; Fisher, K. J.; Gadd, G. E.; Dance, I. G.; Smith, D. R.; Willett, G. D. *Int. J. Mass Spectrom. Ion Processes* **1997**, *164* (1−2), 45.

(12) Dai, D.; Balasubramanian, K. *J. Chem. Phys.* **1996**, *105*, 5901.

(13) Balasubramanian, K. *Chem. Rev.* **1990**, *90*, 93.

(14) Dixon, D. A.; Gole, J. L. *Chem. Phys. Lett.* **1992**, *188*, 560.

(15) Lanza, G.; Millefiori, S.; Millefiori, A. *J. Chem. Soc., Faraday Trans.* **1993**, *89* (16), 2961.

(16) Archibong, E. F.; St-Amant, A. *J. Chem. Phys.* **1998**, *109* (3), 962.

(17) Deutsch, P. W.; Curtiss, L. A.; Blaudeau, J. P. *Chem. Phys. Lett.* **1997**, *270* (5−6), 413.

(18) Ogut, S.; Chelikowsky, J. R. *Phys. Rev. B (Condens. Matter)* **1997**, *55* (8), R4914.

(19) Streitwieser, A.; Bachrach, S. M.; Schleyer, P. v. R. In *Lithium Chemistry- A theoretical and Experimental Overview*; Sapse, A. A., Schleyer, P. v. R., Eds.; Wiley: New York, 1995.

(20) Rappoport, Z.; Marek, I. *The Chemistry of Organolithium Compunds 1*; Jonh Wiley & Sons: New York, 2004.

(21) Gopakumar, G.; Lievens, P.; Nguyen, M. T. *J. Chem. Phys.* **2006**, *124*, 214312.

(22) Schmidt, M. W.; Gordon, M. S. *Annu. Rev. Phys. Chem.* **1998**, *49*, 233.

(23) Nakano, H. J. *Chem. Phys. Lett.* **1993**, *99*, 7983.

(24) Hirao, K. *Chem. Phys. Lett.* **1992**, *196*, 397. Hirao, K. *Chem. Phys. Lett.* **1992**, *190*, 374. Hirao, K. *Chem. Phys. Lett.* **1993**, *201*, 59.

(25) Brandow, B. H. *Int. J. Quant. Chem.* **1979**, *15*, 207. Brandow, B. H. *Rev. Mod. Phys.* **1967**, *39*, 771. Schucan, T. H.; Weidenmuller, H. *Ann. Phys.* **1972**, *73*, 108. Schucan, T. H.; Weidenmuller, H. *Ann. Phys.* **1973**, *76*, 483. Witek, H. A.; Choe, Y. K.; Finley, J. P.; Hirao, K. J. *J. Comput. Chem.* **2002**, *23*, 957.

(26) Frisch, M. J.; Trucks, G. W.; Schlegel, H. B.; Scuseria, G. E.; Robb, M. A.; Cheeseman, J. R.; Montgomery, J. A., Jr.; Vreven, T.; Kudin, K. N.; Burant, J. C.; Millam, J. M.; Iyengar, S. S.; Tomasi, J.; Barone, V.; Mennucci, B.; Cossi, M.; Scalmani, G.; Rega, N.; Petersson, G. A.; Nakatsuji, H.; Hada, M.; Ehara, M.; Toyota, K.; Fukuda, R.; Hasegawa, J.; Ishida, M.; Nakajima, T.; Honda, Y.; Kitao, O.; Nakai, H.; Klene, M.; Li, X.; Knox, J. E.; Hratchian, H. P.; Cross, J. B.; Bakken, V.; Adamo, C.; Jaramillo, J.; Gomperts, R.; Stratmann, R. E.; Yazyev, O.; Austin, A. J.; Cammi, R.; Pomelli, C.; Ochterski, J. W.; Ayala, P. Y.; Morokuma, K.; Voth, G. A.; Salvador, P.; Dannenberg, J. J.; Zakrzewski, V. G.; Dapprich, S.; Daniels, A. D.; Strain, M. C.; Farkas, O.; Malick, D. K.; Rabuck, A. D.; Raghavachari, K.; Foresman, J. B.; Ortiz, J. V.; Cui, Q.; Baboul, A. G.; Clifford, S.; Cioslowski, J.; Stefanov, B. B.; Liu, G.; Liashenko, A.; Piskorz, P.; Komaromi, I.; Martin, R. L.; Fox, D. J.; Keith, T.; Al-Laham, M. A.; Peng, C. Y.; Nanayakkara, A.; Challacombe, M.; Gill, P. M. W.; Johnson, B.; Chen, W.; Wong, M. W.; Gonzalez, C.; Pople, J. A. *Gaussian 03*, revision C.01; Gaussian, Inc.: Wallingford, CT, 2004.

(27) Schmidt, M. W.; Baldridge, K. K.; Boatz, J. A.; Elbert, S. T.; Gordon, M. S.; Jensen, J. H; Koseki, S.; Matsunaga, N.; Nguyen, K. A.; Su, S. J.; Windus, T. L.; Dupuis, M.; Montgomery, J. A. *J. Comput. Chem. Phys.* **1993**, *14*, 1347. GAMESS program.

(28) Biegler-König, F.; Schönbohm, J.; Bayles, D. AIM2000 - A Program to Analyze and Visualize Atoms in Molecules. *J. Comput. Chem.* **2001**, *22*, 545.

(29) Noury, S.; Krokidis, X.; Fuster, F.; Silvi, B. TopMod package, Université Pierre et Marie Curie, Paris, 1998.

(30) Xu, W. G.; Zhao, Y.; Li, Q. S.; Xie, Y. M.; Schaefer, H. F. *Mol. Phys.* **2004**, *102*, 579.

(31) Burton, G. R.; Xu, C.; Arnold, C. C.; Neumark, D. M. *J. Chem. Phys.* **1996**, *104* (8), 2757. Dai, D.; Sumathi, K.; Balasubramanian, K. *Chem. Phys. Lett.* **1992**, *193*, 251. Dixon, D. A.; Gole, J. L. *Chem. Phys. Lett.* **1992**, *188*, 560.

(32) Bader, R. F. *Atoms in Molecules A Quantum Theory*; Oxford University Press: Oxford, U.K., 1995.

(33) Popellier, P. *Atoms in Molecules An Introduction*; Prentice Hall: Englewood Cliffs, NJ, 2000.

(34) Ponec, R.; Roithova, J.; Girones, X.; Lain, L.; Torre, A.; Bochicchio, R.; *J. Phys. Chem. A* **2002**, *106*, 1019.

(35) Silvi, B.; Savin, A. *Nature* **1994**, *371*, 683.

(36) Laaksonen, L. J. *J. Mol. Graph.* **1992**, *10*, 33. Bergman, D. L.; Laaksonen, L.; Laaksonen, A. *J. Mol. Graph. Model.* **1997**, *15*, 301.

(37) Kohout, M.; Wagner, F.R.; Grin, Y. *Theor. Chem. Acc.* **2002**, *108*, 150.